Synthesis of interstellar 1,3,5-heptatriynylidyne, $C_7H(X\,^2\Pi)$, via the neutral-neutral reaction of ground state carbon atom, $C(^3P)$, with triacetylene, HC_6H $(X\,^1\Sigma_g^+)$

B. J. Sun,[1] C. H. Huang,[1] M. F. Tsai,[1] H. L. Sun,[1] L. G. Gao,[1] Y. S. Wang,[1] Y. Y. Yeh,[1] Y. H. Shih,[1] Z. F. Sia,[1] P. H. Chen,[1] R. I. Kaiser,[2] and A. H. H. Chang[1,a)]
[1]*Department of Chemistry, National Dong Hwa University, Shoufeng, Hualien 974, Taiwan*
[2]*Department of Chemistry, University of Hawaii at Manoa, Honolulu, Hawaii 96822, USA*

(Received 6 June 2009; accepted 4 August 2009; published online 11 September 2009)

The reaction of ground-state carbon atom with a polyyne, triacetylene (HC_6H) is investigated theoretically by combining *ab initio* calculations for predicting reaction paths, RRKM theory to yield rate constant for each path, and a modified Langevin model for estimating capturing cross sections. The isomerization and dissociation channels for each of the five collision complexes are characterized by utilizing the unrestricted B3LYP/6-311G(d,p) level of theory and the CCSD(T)/cc-pVTZ calculations. Navigating with the aid of RRKM rate constants through web of *ab initio* paths composed of 5 collision complexes, 108 intermediates, and 20 H-dissociated products, the most probable paths, reduced to around ten species at collision energies of 0 and 10 kcal/mol, respectively, are identified and adopted as the reaction mechanisms. The rate equations for the reaction mechanisms are solved numerically such that the evolutions of concentrations with time for all species involved are obtained and their lifetimes deduced. This study predicts that the five collision complexes, c1–c5, would produce a single final product, C_7H (p1)+H, via the most stable intermediate, carbon chain HC_7H (i1); namely, $C+HC_6H \rightarrow HC_7H \rightarrow C_7H+H$. Our investigation indicates that the title reaction is efficient to form astronomically observed C_7H in cold molecular clouds, where a typical translational temperature is 10 K. © *2009 American Institute of Physics*. [doi:10.1063/1.3212625]

I. INTRODUCTION

Carbon chain molecules represent a significant fraction of those 150 detected molecules in the interstellar medium and circumstellar envelope of carbon stars.[1] The largest observed interstellar molecule,[2] the linear $HC_{11}N$ species, is a member of cyanopolyyne family, in which $HC_{2n+1}N$ ($n=1-5$) have been observed.[3–6] Also, C_nH ($n=1-8$) radicals are detected[7–14] in dark molecular clouds via radioastronomy. On the other hand, none of the nonpolar $HC_{2n+1}H$ ($n=1,2\cdots$) has been detected in space so far; through infrared spectroscopy two polyynes, HC_4H and HC_6H, are tentatively located[15] in planetary nebulae. In spite of notably higher energy, their isomers, three cumulene carbenes, H_2C_3, H_2C_4, and H_2C_6, are readily observed[16–18] with radio telescopes since they possess dipole moments; the rotational spectra of H_2C_5, H_2C_7, H_2C_8, H_2C_9, and D_2C_{10} are obtained in the laboratory.[19–21] It is widely believed that the unobserved symmetric HC_nH molecules are present in the regions where their analogs are found.

Why are these carbon chain molecules important? Carbon chain molecules and their ions have long been suspected[22,23] as carriers of DIBs (the diffuse interstellar bands),[24] the mysterious hundreds of absorption lines in visible regions. Thus multiple laboratory investigations on the electronic absorption spectra of carbon chain molecules have been carried out: $HC_{2n}H$ up to impressively long $HC_{26}H$,[25] the less stable $HC_{2n+1}H$ ($n=3-6,9$),[26–28] C_nH [29–32] up to $n=10$, and the protonated polyynes, $HC_{2n}H_2^+$($n=3,4$).[33] The C_4H radical is studied via laser induced fluorescence.[34] Nevertheless, for eight decades since the discovery[35] of DIBs, not a single molecule matches definitely, whose size is speculated being of 10–50 atoms;[36,37] the assignment[38] of C_7^-, however, is controversial.[39,40]

As microwave, infrared, and electronic spectroscopies could establish the presence and abundance of astronomical molecules, chemical models[41–44] serve to explain the relations among them and the observed abundances. The prototype $C(^3P)+C_2H_2$ (acetylene) reaction[45,46] has been intensively studied experimentally and theoretically, since the neutral-neutral reactions[47,48] between atomic carbon and unsaturated hydrocarbons are considered an important synthetic route to complex molecules in interstellar medium. Recently, we examined[49,50] the reaction next in line, $C(^3P)+HC_4H$ (diacetylene). The reaction of carbon atom with the polyynes, $HC_{2n}H$, could also be viewed as a mechanism for the formation of $C_{2n+1}H$ and $HC_{2n+1}H$ isomers and thus the depletion of the polyynes. Together, the first two members seemingly open a reaction class of $C(^3P)+HC_{2n}H \rightarrow HC_{2n+1}H \rightarrow C_{2n+1}H+H$, where the vital intermediate $HC_{2n+1}H$ and product $C_{2n+1}H$ are found[49] exclusively long-chained particularly when $n=2$. Recall that the reaction of ground state

a)Electronic mail: hhchang@mail.ndhu.edu.tw. FAX: +886-3-8633570.

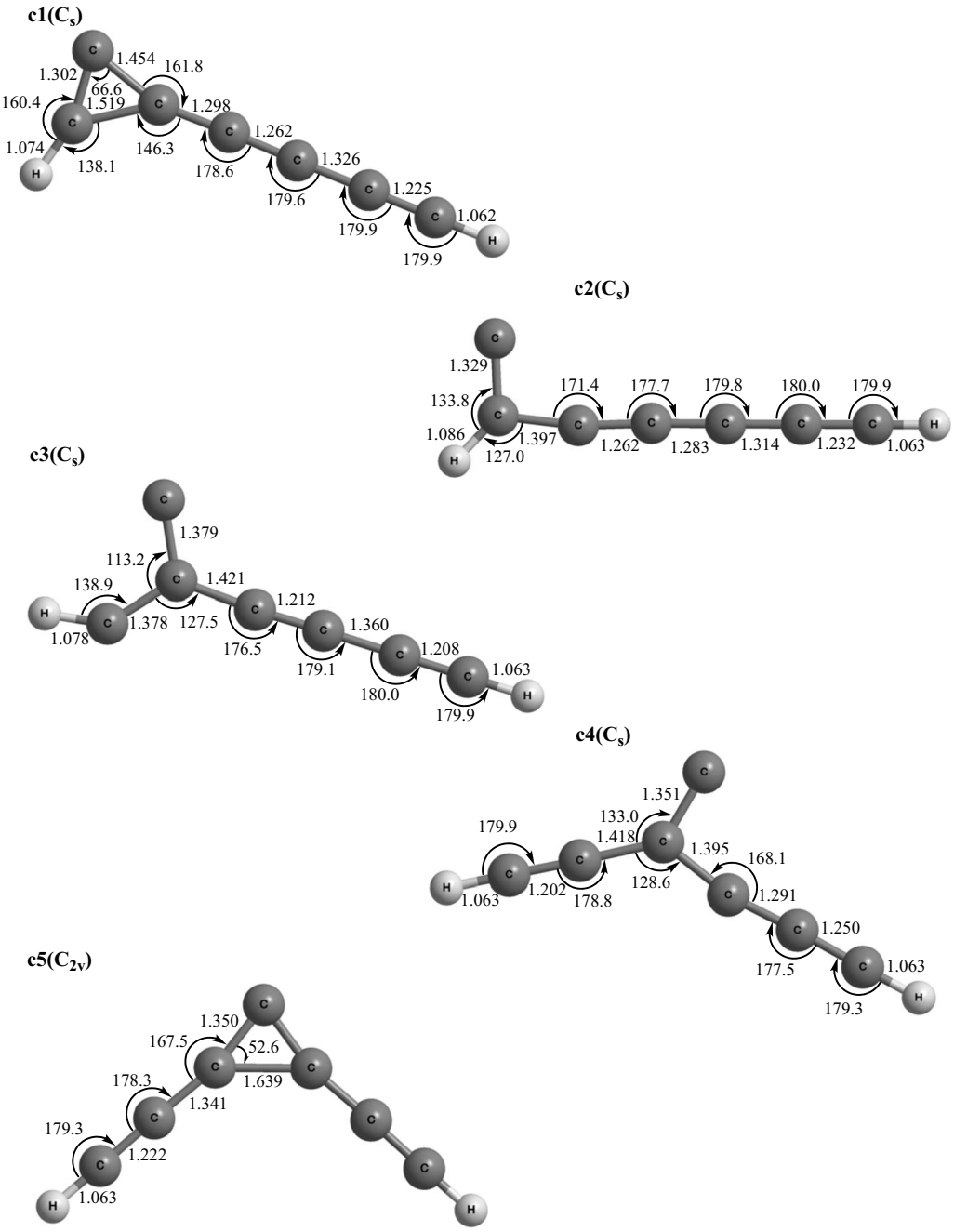

FIG. 1. The B3LYP/6-311G(d,p) optimized geometries of the five collision complexes of the $C(^3P)+HC_6H(X\ ^1\Sigma_g^+)$ reaction, in which the point group is in parenthesis, lengths are in angstrom, and the angles are in degree.

carbon atoms with acetylene also forms a cyclic C_3H isomer; likewise, in this reaction, the tricarbon plus molecular hydrogen channel is open as well. It is desirable to study the third member of the sequence, $C(^3P)+HC_6H$ (triacetylene), not only because the reaction is likely to be as fast as the other two, but also to see whether the same simple mechanism holds or more stable ringed isomers are formed.

Various *ab initio* calculations have been performed on the singlet,[51,52] triplet,[28,51–56] and excited[28,54,56] triplet states of linear HC_7H and isomers[51–55,57] mostly in singlet state and C_7H isomers.[32,51,58,59] However, previous theoretical efforts mainly tackle the properties of individual molecules. In this work, a theoretical study is set out to acquire the reaction mechanism and dynamics of the $C(^3P)+HC_6H$ $(X\ ^1\Sigma_g^+)$ reaction, in which intricate interplays among interstellar molecules, HC_7H, C_7H, and their isomers, could be realized. Our aim is to first identify through *ab initio* calculations the exoergic channels without entrance barrier, which would be competitive and relevant for the very low temperature and density in dense interstellar clouds; second, to derive the energy dependent reaction mechanism by computing the RRKM rate constants of elementary steps specifically tuned for the condition of single binary collision; subsequently, to obtain concentration evolutions with time for intermediates and products during the reaction by solving the rate equations for the reaction mechanism; finally, to predict the product abundances at different collision energies.

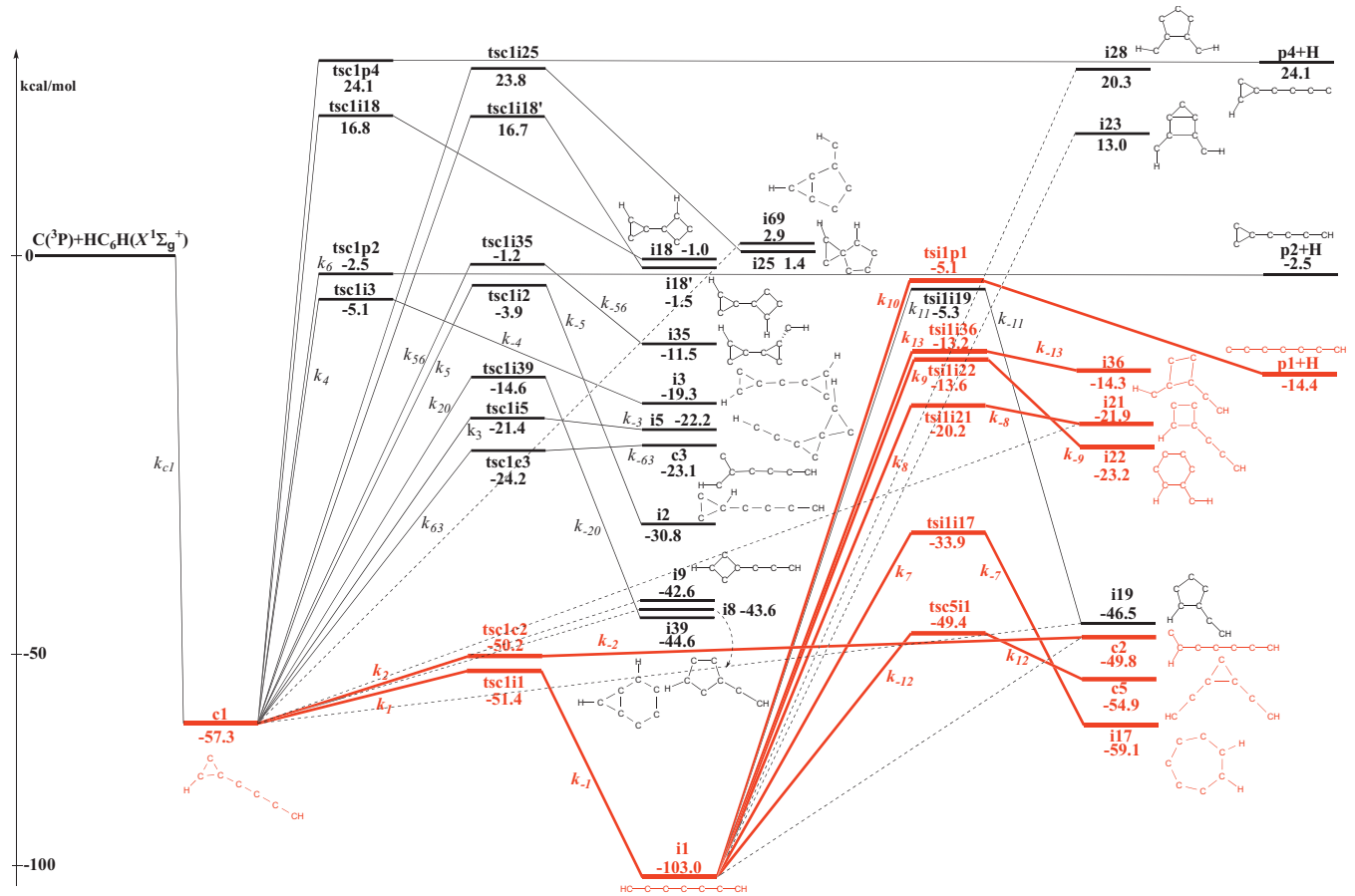

FIG. 2. The reaction paths and the most probable paths (highlighted) at zero collision energy of the collision complex, c1, in which the energies are computed with CCSD(T)/cc-pVTZ level of theory with B3LYP/6-311G(d,p) zero-point energy corrections at the B3LYP/6-311G(d,p) optimized geometries. Note that, for those paths in dotted lines, the attempts are not made or not successful in locating the transition states.

II. THEORETICAL METHODS

A. *Ab initio* electronic structure calculations: Reaction paths prediction

The paths of the C(^3P)+HC$_6$H ($X\ ^1\Sigma_g^+$) reaction under single collision are inferred theoretically. The reaction is assumed to proceed on the adiabatic triplet ground-state potential energy surface of C$_7$H$_2$. When the multiple π systems of triacetylene attacked by carbon atoms, it is expected to yield multiple collision complexes. Therefore, possible collision complexes are first identified, followed by the characterization of low-energy isomerization channels for each collision complex. The optimized geometries and harmonic frequencies of intermediates, transition states, and dissociation products are obtained at the level of the hybrid density functional theory, the unrestricted B3LYP[60]/6-311G(d,p), with energies further refined by the coupled cluster[61] CCSD(T)/cc-pVTZ with unrestricted B3LYP/6-311G(d,p) zero-point energy corrections. The locations of variational transition state geometries for C(^3P)+HC$_6$H($X\ ^1\Sigma_g^+$) reaction that lead to the collision complexes are facilitated by intrinsic reaction coordinate (IRC) calculations at unrestricted B3LYP/6-311G(d,p) level of theory along the breaking C–C bonds of respective collision complexes. The GAUSSIAN98 and 03 programs[62] are employed for the electronic structure calculations.

B. RRKM and variational RRKM theory: Rate constant calculations

Assuming the energy is equilibrated among molecular degrees of freedom when the reaction occurs, the rate of reaction can be described statistically. Provided the energy is conserved during the reaction such as in low-density environments or molecular beam experiments where condition for single collision is warranted, the rate constant could be predicted by RRKM theory. That is, for a unimolecular reaction $A^* \xrightarrow{k} A^{\neq} \rightarrow P$, where A^* is the energized reactant, $A^{\neq}$ represents the transition state, and P the products, the rate constant $k(E)$ may be expressed as

$$k(E) = \frac{\sigma}{h}\frac{W^{\neq}(E-E^{\neq})}{\rho(E)}, \tag{1}$$

where σ is the symmetry factor, $W^{\neq}$ is the number of states of the transition state, $E^{\neq}$ is the transition state energy, and ρ is the density of states of the reactant. In this work, ρ and $W^{\neq}$ are computed by saddle-point method[63,64] and molecules are treated as collections of harmonic oscillators whose harmonic frequencies are obtained as described in Sec. II A.

As the formation of collision complexes from C(^3P)+HC$_6$H is barrierless, there will also be no barrier to the reverse redissociation of the complexes. For a barrierless reaction as such, kinetic equivalence to the saddle point on the

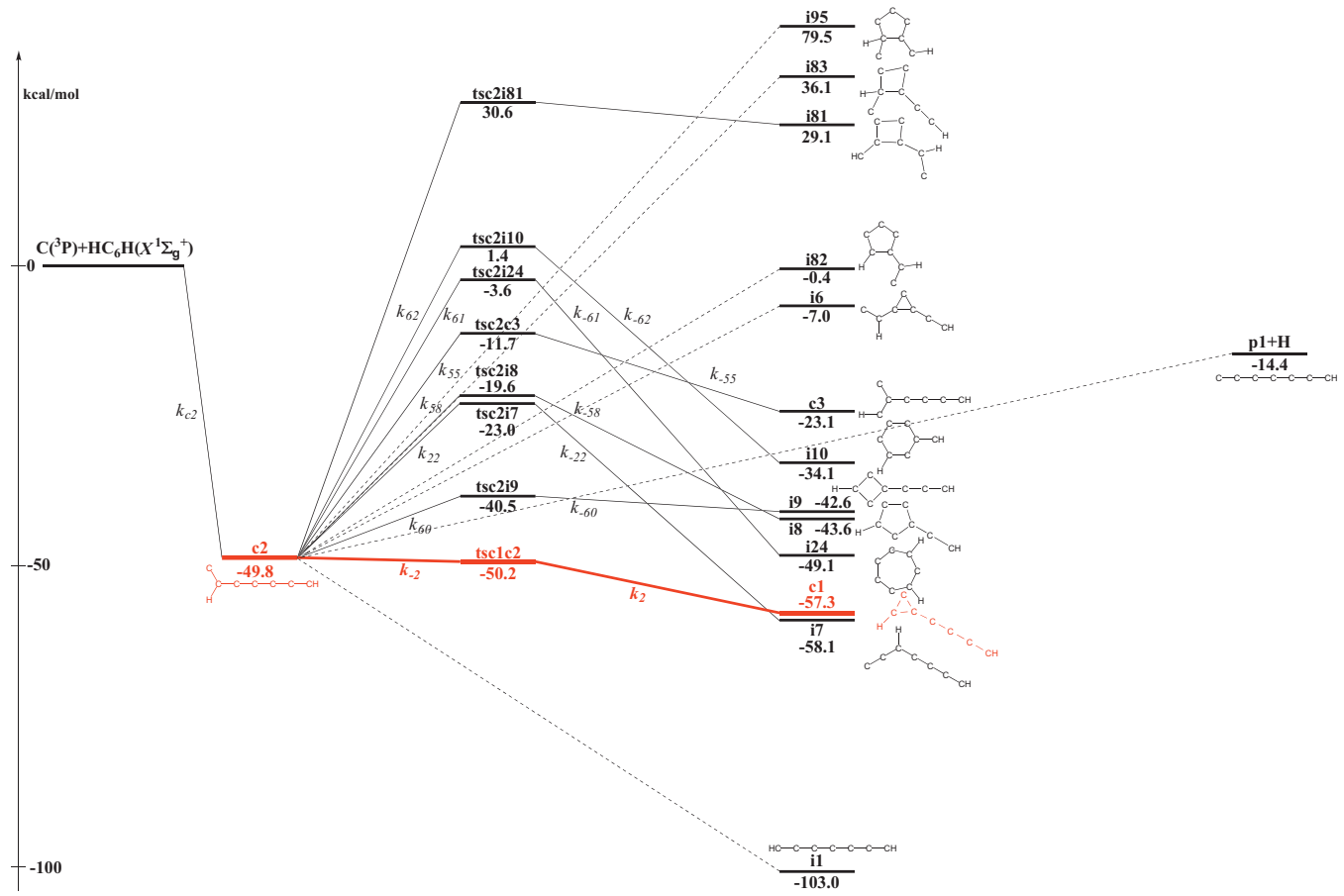

FIG. 3. The reaction paths and the most probable paths (highlighted) at zero collision energy of the collision complex, c2, in which the energies are computed with CCSD(T)/cc-pVTZ level of theory with B3LYP/6-311G(d,p) zero-point energy corrections at the B3LYP/6-311G(d,p) optimized geometries. Note, for those paths in dotted lines, that the attempts are not made or not successful in locating the transition states.

potential energy surface, the geometry of minimum flux, could be adopted as transition state. Specifically, the variational transition state is located when (e.g., Refs. 65–67)

$$\frac{\partial W(E,R)}{\partial R} = 0, \tag{2}$$

where W is the number of states and R is the reaction coordinate, breaking C–C bond in this case. The variational transition states are apparently both energy and reaction-coordinate dependent. Once the transition state is variationally determined for each collision complex at each of the six collision energies (0.0, 0.03, 0.15, 2.0, 5, and 10 kcal/mol, which correspond to average kinetic energies of an ideal gas molecule at temperatures of 0, 10, 50, 671, 1678, and 3355 K, respectively), the RRKM rate constant $k(E)$ for collision complex $\rightarrow C(^3P)+HC_6H$ could be computed according to Eq. (1).

C. Solution of the rate equations: Evolution with time and branching ratios

The rate equations for reaction mechanism of each collision complex are solved by the numerical Runge–Kutta method at collision energies of 0 and 10 kcal/mol. The solutions yield the concentrations of species in the reaction mechanisms as a function of time; that is, the concentration evolution with time. The branching ratio could be easily derived from the asymptotic values.

D. Reaction cross sections for the formation of collision complexes

With the branching ratio resolved within the mechanism of each collision complex as explained above, the branching ratio for the title reaction could be realized when the reaction cross sections for forming all collision complexes are known. For a barrierless reaction, the capturing cross section derived by the simple Langevin model would be $\sigma(E) \propto (C/E)^{1/3}$, where E is the collision energy, if the intermolecular potential between reactants is approximated by a long-range form, $V(R) = -C/R^s$, where $s=6$ when both reactants are nonpolar, C is a constant, and R is the distance between centers of mass of two reactants. The complication multiplies for a nine-atomic system, of which the potential energy surface is a formidable 21 dimensional function of internal degrees of freedom. The fact that there are multiple collision complexes for the $C+HC_6H$ reaction signifies that the reaction cross section for this bimolecular reaction is orientation dependent.

As devised in the $C+HC_4H$ reaction,[49] the 21 dimensional potential surface near the entrance of the reaction is reduced to five one-dimensional curves, which are conveniently adopted from the same IRC results in Sec. II A and

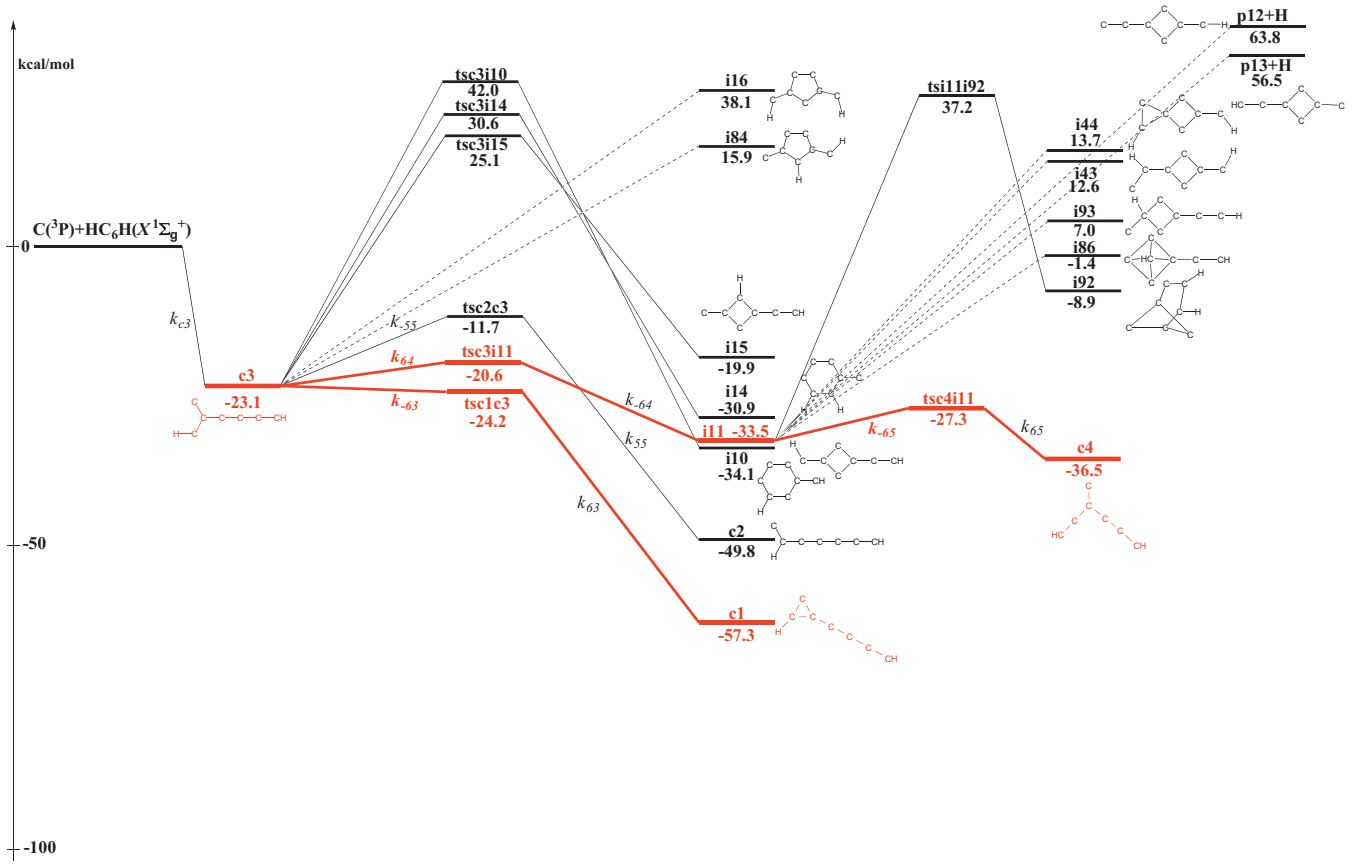

FIG. 4. The reaction paths and the most probable paths(highlighted) at zero collision energy of the collision complex, c3, in which the energies are computed with CCSD(T)/cc-pVTZ level of theory with B3LYP/6-311G(d,p) zero-point energy corrections at the B3LYP/6-311G(d,p) optimized geometries. Note, for those paths in dotted lines, that the attempts are not made or not successful in locating the transition states.

where the orientation dependence is implicitly incorporated, corresponding to formation paths of the five collision complexes, respectively. Specifically, one-dimensional potential energy curves, V_1, V_2, V_3, V_4, and V_5, are thus defined along the reaction coordinates, R_1, R_2, R_3, R_4, and R_5, of C $+HC_6H \rightarrow$ collision complex 1, $C+HC_6H \rightarrow$ collision complex 2, $C+HC_6H \rightarrow$ collision complex 3, $C+HC_6H \rightarrow$ collision complex 4, and $C+HC_6H \rightarrow$ collision complex 5, respectively. The asymptotic portions of $V_1(R_1), V_2(R_2), V_3(R_3), V_4(R_4), V_5(R_5)$ are least-squares fitted into $-C(1)/R_1^6$, $-C(2)/R_2^6$, $-C(3)/R_3^6$, $-C(4)/R_4^6$, $-C(5)/R_5^6$ to obtain the constants, $C(1)$, $C(2)$, $C(3)$, $C(4)$, and $C(5)$, respectively. Applying the Langevin model,[68] the ratio of cross sections forming collision complexes would be $\sigma_{c1}:\sigma_{c2}:\sigma_{c3}:\sigma_{c4}:\sigma_{c5}=C(1)^{1/3}:C(2)^{1/3}:C(3)^{1/3}:C(4)^{1/3}:C(5)^{1/3}$.

III. RESULTS AND DISCUSSION

The barrierless attack of electrophilic carbon atom to the π systems of triacetylene molecule could readily trigger the $C(^3P)+HC_6H(X\ ^1\Sigma_g^+)$ reaction. Each binary collision of reactants, $C(^3P)$ and $HC_6H(X\ ^1\Sigma_g^+)$, yields one collision complex. Five collision complexes are characterized and denoted as c1, c2, c3, c4, and c5; their B3LYP/6-311G(d,p) optimized geometries are illustrated in Fig. 1.

The reaction paths of the titled reaction are assembled by independently following the routes for individual collision complex. The immediate channels of c1–c5, respectively, are identified, which consist of low-energy isomerizations of hydrogen shift, carbon shift, ring formation, ring opening, carbon decomposition, and hydrogen atom elimination. The rate constants for all the immediate paths with energy under10 kcal/mol (relative to the reactants) are then estimated. A simple scheme is adopted to sensibly avoid escalating the number of paths, in which the computed rate constants facilitate in navigating through the web of reaction channels: only the immediate channels for those intermediates produced with the largest rate constants, or equivalently along the most kinetically competitive paths, are tracked further. The pursuit of reaction paths was aborted when the dissociation is encountered.

The B3LYP/6-311G(d,p) optimized structures of intermediates, dissociation products, and transition states, designated as i, p, and ts are drawn in Figs. s1, s2, and s3,[69] respectively; their predicted energies are listed in Table s1[69] and the energy-dependent rate constants of elementary steps computed at collision energies of 0.0, 0.03, 0.15, 2.0, 5, and 10 kcal/mol in Table s2.[69] The CCSD(T)/cc-pVTZ energetic paths of c1–c5 determined are plotted in Figs. 2–6, respectively. Correspondingly, the reaction mechanisms inferred at collision energy of 0 and 10 kcal/mol are drafted in Figs. 7 and 8, respectively. In the discussion that follows, the energies cited are the CCSD(T)/cc-pVTZ energies relative to the

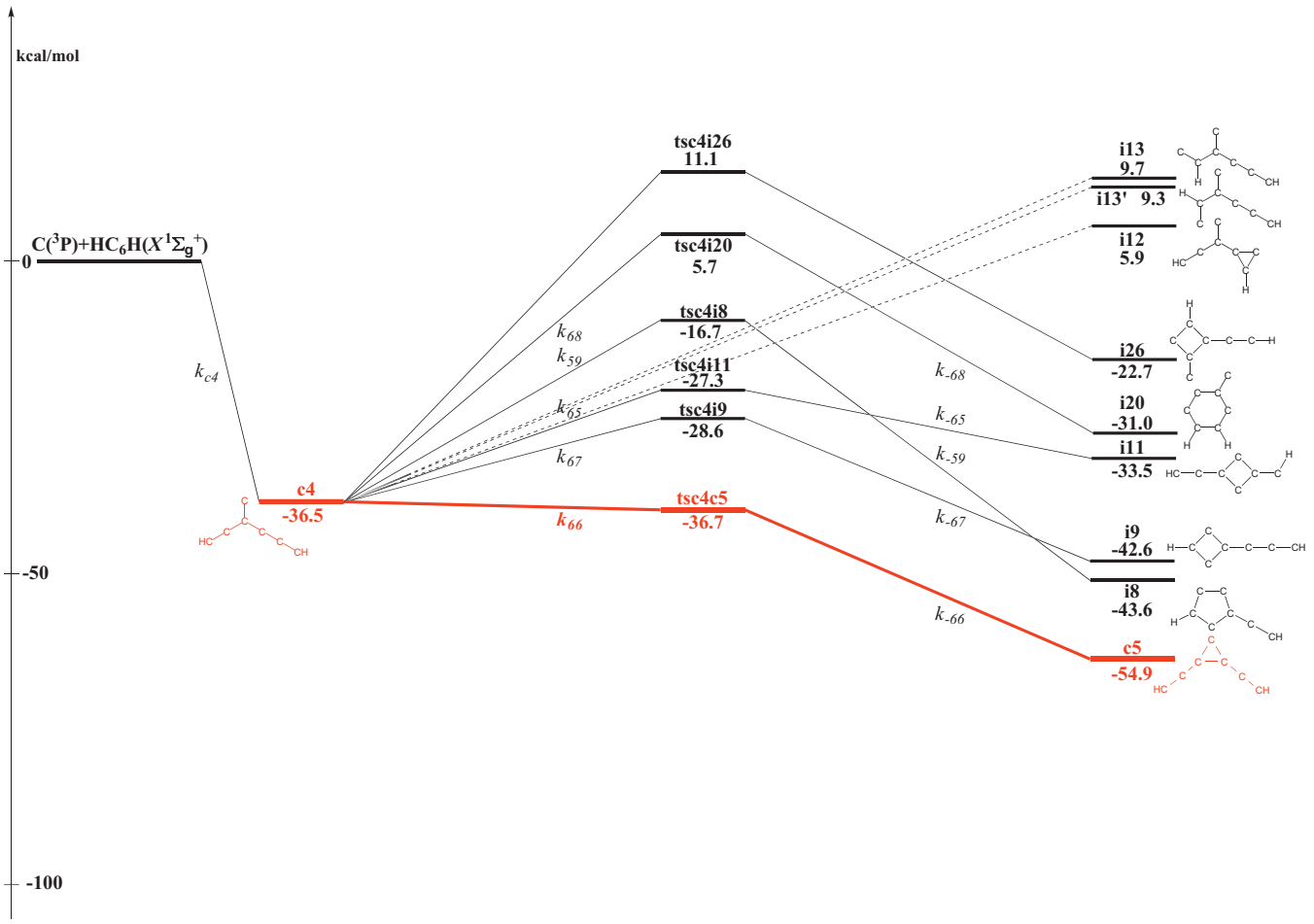

FIG. 5. The reaction paths and the most probable paths(highlighted) at zero collision energy of the collision complex, c4, in which the energies are computed with CCSD(T)/cc-pVTZ level of theory with B3LYP/6-311G(d,p) zero-point energy corrections at the B3LYP/6-311G(d,p) optimized geometries. Note, for those paths in dotted lines, that the attempts are not made or not successful in locating the transition states.

reactants with B3LYP/6-311G(d,p) zero-point energy corrections and the quoted rate constants are computed at zero collision energy if not otherwise stated.

A. Dissociation of collision complex back to reactants, C+HC$_6$H

As tabulated in Table s1, all five collision complexes are comfortably bound relative to the reactants with c1 sinking as deep as −57.3 kcal/mol and c3 the least stable at −23.1 kcal/mol. The energy-dependent transition states, tsc1–tsc5, for the carbon dissociations, c1→C+HC$_6$H, c2→C+HC$_6$H, c3→C+HC$_6$H, c4→C+HC$_6$H, and c5→C+HC$_6$H, respectively, are determined with the aid of variational RRKM theory at six collision energies (0.0, 0.03, 0.15, 2.0, 5.0, and 10.0 kcal/mol), which gives an overall 30 transition states. As collision energy increases from 0.0 to 10 kcal/mol, their geometries in Fig. s3 indicate that the leaving C–C separations fall within 4.6–3.7, 3.8–3.5, and 4.1–3.4, 3.8–3.3, and 4.3–3.5 Å for tsc1–tsc5, respectively, with the corresponding energies located at −0.3 to −0.9, −0.8 to −1.0, −0.7 to −1.3, −1.0 to −1.5, and −0.4 to −1.1 kcal/mol, which is reasonable for their reactantlike geometries. The trend is in line with the anticipation that transition state gets tighter (i.e., shorter C–C distance) and its energy is descending with higher collision energy. At each of the six collision energies, the five transition state energies are well within 1 kcal/mol apart—essentially equal; thus the more stable collision complex would encounter larger activation energy. The phenomenon is demonstrated rather nicely by the predicted rate constants in Table s2, which follow the order of $k_{c1}<k_{c5}<k_{c2}<k_{c4}<k_{c3}$ through out the collision energies of 0–10 kcal/mol as the stability of the collision complexes, c1>c5>c2>c4>c3, would implicate. Evidently, the least stable c3 is most ready to release a carbon atom.

B. Dissociation products

The energies of twenty C$_7$H species, which are relevant hydrogen-dissociation products, are listed in Table s1 and their geometries displayed in Fig. s2. Analogous to the C$_5$H isomers, the linear 1,3,5-heptatriynylidyne (p1) is more stable than the three-member ringed 1,4-butadiynylcyclopropendiylidene (p2). With energies predicted to be −14.4 and −2.5 kcal/mol, respectively, p1+H and p2+H are the only dissociation products with energy lower than the reactants. The rest of the C$_7$H isomers are however substantially higher in energy and expectedly out of reach at ultralow temperature.

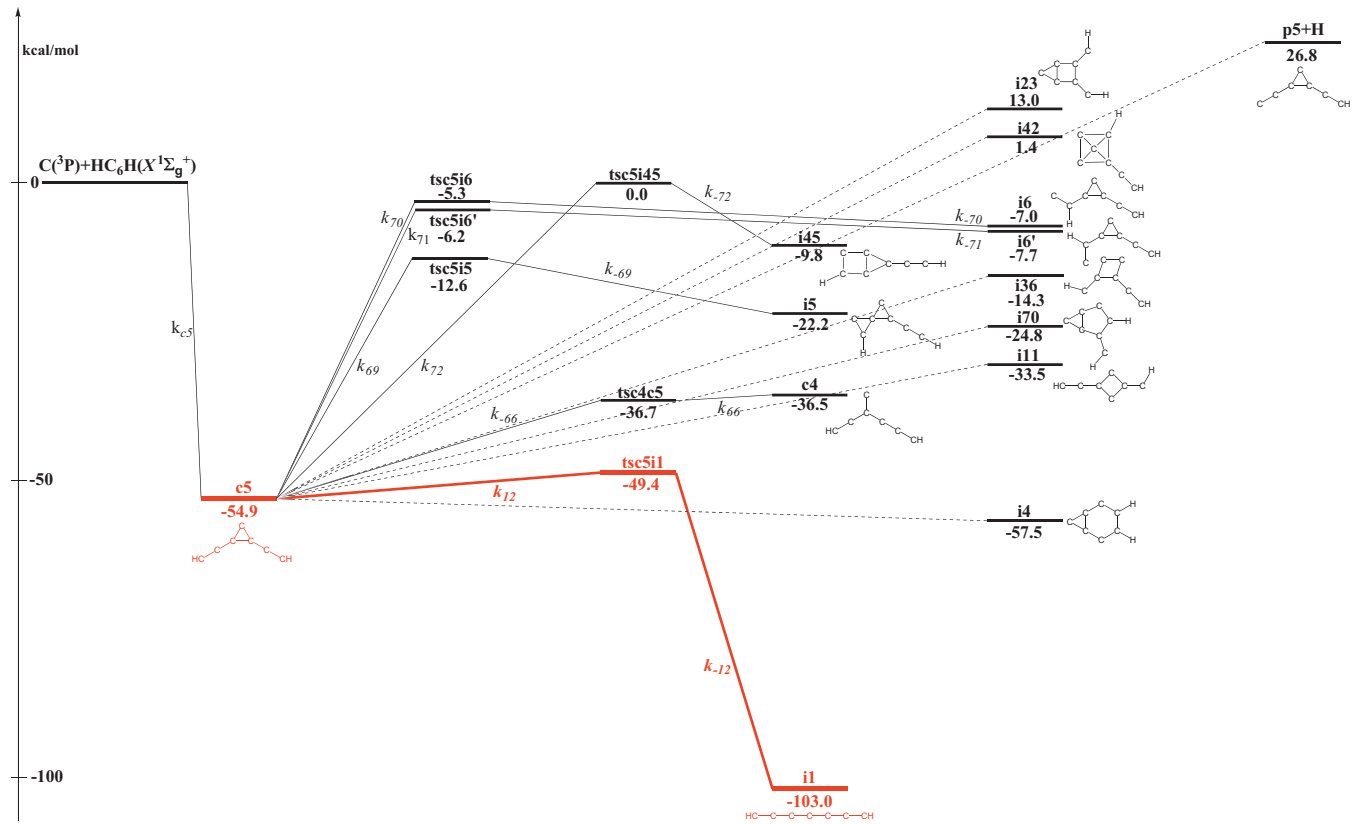

FIG. 6. The reaction paths and the most probable paths(highlighted) at zero collision energy of the collision complex, c5, in which the energies are computed with CCSD(T)/cc-pVTZ level of theory with B3LYP/6-311G(d,p) zero-point energy corrections at the B3LYP/6-311G(d,p) optimized geometries. Note, for those paths in dotted lines, that the attempts are not made or not successful in locating the transition states.

Among three C_7 products that might be formed by H_2 elimination, the seven member ringed p20 has a near reactant energy of 0.3 kcal/mol, seemingly energetically accessible even at low temperature, and would in fact be eliminated kinetically as reasoned in the following sections. The other two H_2-dissociations and the feasibility of CH and CH_2 eliminations could be easily ruled out judging from their probable product energies being 24.2 kcal/mol and above as listed in Table s1.

C. Reaction paths and the most probable paths of collision complex c1

As seen in Fig. 2, there could be fourteen low energy channels for c1: three ring openings to i1(hept-2,3,4,5-tetraene-1,6-diyne), c2, and c3, one 1,2 H-shift to i2, seven ring formations to i39, i5, i3, i35, i18, i25, and i69, one carbon dissociation back to reactants, and two H-dissociations to p2 and p4. Among them, the paths of c1 →i1 and c1→c2 encounter much lower barriers of 5.9 and 7.1 kcal/mol, respectively, than the third lowest activation energy, 33.1 kcal/mol, for c1→c3. The trend persists kinetically as the RRKM rate constant calculations give 3.92×10^{12} and 2.29×10^{12} s^{-1} for k_1 (c1→i1) and k_2 (c1 →c2), respectively, and a trailing k_{63} (c1→c3), 3.56×10^7 s^{-1}.

Only the channels of kinetically prevailed intermediates, c2 and i1, are traced further. c2 most likely undergoes ring closing back to c1 as discussed below. The most energetically stable intermediate, the chained i1, could form a three-member ring back to c1, cyclize to i17, c5, i19, i21, i22, i23, i28, i36, and eliminate hydrogen atom to yield p1. The conversion of i1 to c2 through a 1,2 H-shift seems not likely since the transition state could not be found despite many attempts. Overall, ten available channels are characterized for i1, in which the comparable k_{-1} (i1→c1) and k_{-12} (i1 →c5) estimated to be 8.01×10^7 and 3.21×10^7 s^{-1}, respectively, are dominate considering the third largest rate constant k_7 (i1→i17) for i1 are three order less. However, as i1 follows the leading rate constants and isomerizes to c1 and c5, c1 would rush right back at i1 and likewise for c5 whose paths are scrutinized in a section below. Thus i1 should look for the next probable path for dissipation, namely, a seven-member ring formation to i17. The analysis of channels for the latter detailed in Fig. s4[69] indicates again that its reversed reaction to i1 is the most probable. The i1 channels next in line in the order of decreasing rate constants, i1→i21 ($k_8 = 2.16 \times 10^2$ s^{-1}), i1→i36 ($k_{13} = 2.03$ s^{-1}), and i1→i22 ($k_9 = 1.72$ s^{-1}), would encounter similar circumstances that these three intermediates prefer ring opening back to i1, as revealed by the study of their paths in Figs. s5–s7,[69] respectively. Eventually, the build up of i1 concentration could leak through a hydrogen atom dissociation and yield p1+H with the rate constant k_{10} being 0.51 s^{-1}.

Generally speaking, tunneling effects are significant when a hydrogen atom is involved in the reaction coordinate and, particularly, the collision energy is near the energy barrier. Therefore, with tsi1p1 located at −5.1 kcal/mol, the rate

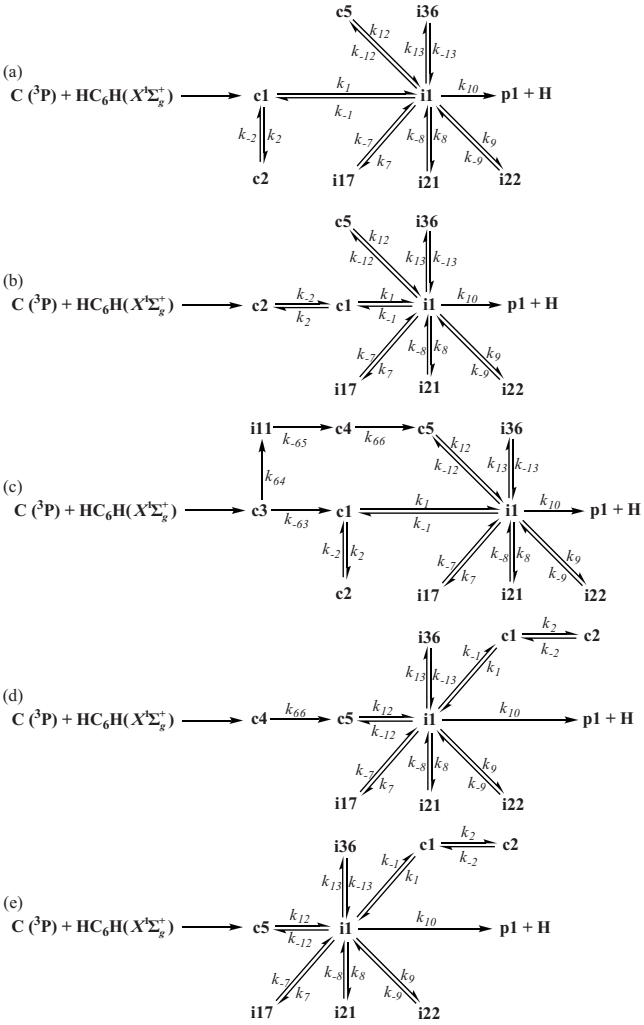

FIG. 7. The reaction mechanisms (a)–(e) derived from the most probable paths at zero collision energy of collision complexes c1–c5, respectively, in which the k are the corresponding rate constants.

constant k_{10} for the hydrogen atom elimination channel of i1, i1→p1+H is expected to be enhanced if tunneling effects are incorporated; however, since p1+H is the only product, its branching ratio would not be affected.

D. Reaction paths and the most probable paths of collision complex c2

Figure 3 demonstrates that the transition states are located for c2 cyclization to three-member ringed c1, four-member ringed i9, five-member ringed i8, six-member ringed i10, and seven-member ringed i24. It is predicted that c2 could also undergo 1,2 H-shift to generate i7, 1,2 C-shift to arrive at c3, and carbon elimination back to reactants. c2 hydrogen dissociation to produce p1 is certainly energetically feasible, however, the transition state could not be identified and locating the product of the other H-elimination is not successful either. It is noted that the branched c2 is rather unstable toward ring closure to c1 as signified by the tsclc2 being slightly lower in energy than c2. It is thus not surprising that the rate constant calculations should give a definite edge to k_{-2} (c2→c1) over the rest of c2 paths.

E. Reaction paths and the most probable paths of collision complex c3

Figure 4 indicates that as a result of c3 four-member ring closure, six-member ring closure, another six-member ring closure, the intermediates, i15, i14 (cyclohexa-1,3-diyne-5-ene-1-ylidenecarbene), and i10 (cyclohexa-1,2,3,4-tetraene-6-yne-1-ylidenemethyl), respectively, though sufficiently bound, are not accessible at low collision energy since the corresponding transition states are at least 25.1 kcal/mol above the reactants C+HC$_6$H. In addition, two immediate intermediates via c3 five-member ring formations, i16 and i84 are identified, however, at not easily reached 38.1 and 15.9 kcal/mol, respectively. It appears that choices of further reaction for the least stable collision complex c3 are rather limited. Only four low energy paths are available for c3: three-member ring-closure to c1, four-member ring formation to i11, 1,2 carbon shift to c2, and carbon dissociation to reactants. The rate constants k_{-63} (c3→c1) and k_{64} (c3→i11) stand out that c3 would proceed to c1 and i11. The latter simply opens its ring to become c4 since with k_{-65} being 1.25×10^{13} s^{-1}, i11→c4 suppresses the other eight i11 channels.

F. Reaction paths and the most probable paths of collision complex c4

Figure 5 shows six channels with transition states characterized for c4: three-member ring closure to c5, four-member ring formations to i9 and i11, to i8 of five-member ring, to the six-member ringed i20, and carbon dissociation to the reactants. In particular, resembling c2 and c3 versus c1, the branched c4 is unstable toward three-member ring closure to yield c5 as suggested by tsc4c5 in a lower energy than c4. Thus the minimum energy path c4→c5 is comfortably being the most probable.

G. Reaction paths and the most probable paths of collision complex c5

The channels for the two ring openings transforming c5 to i1 and c4, 1,2 H-shift to i6, two ring formations to i5 and i45, and carbon elimination to reactants are characterized as presented in Fig. 6. The transition states for further ring formations generating bound intermediates i4, i11, i70, and i36 could not be located. As supported by the rate constant calculations, rather like its fellow collision complex c1, the ringed c5 would swiftly stretch to i1, the immediate destination of c5 minimum energy path.

H. Reaction mechanisms

Zero collision energy. The most probable paths of c1–c5 highlighted in Figs. 2–6, respectively, are determined according to kinetic competitiveness at zero collision energy, specifically, the paths with leading rate constants but not necessarily the minimum energy paths. The most probable paths derived reaction mechanisms are presented in Fig. 7. While the most probable paths illustrated in Figs. 2–6 are emphasized energetically, the complementary Figs. 7(a)–7(e) describe the directions of reaction. The three branched collision

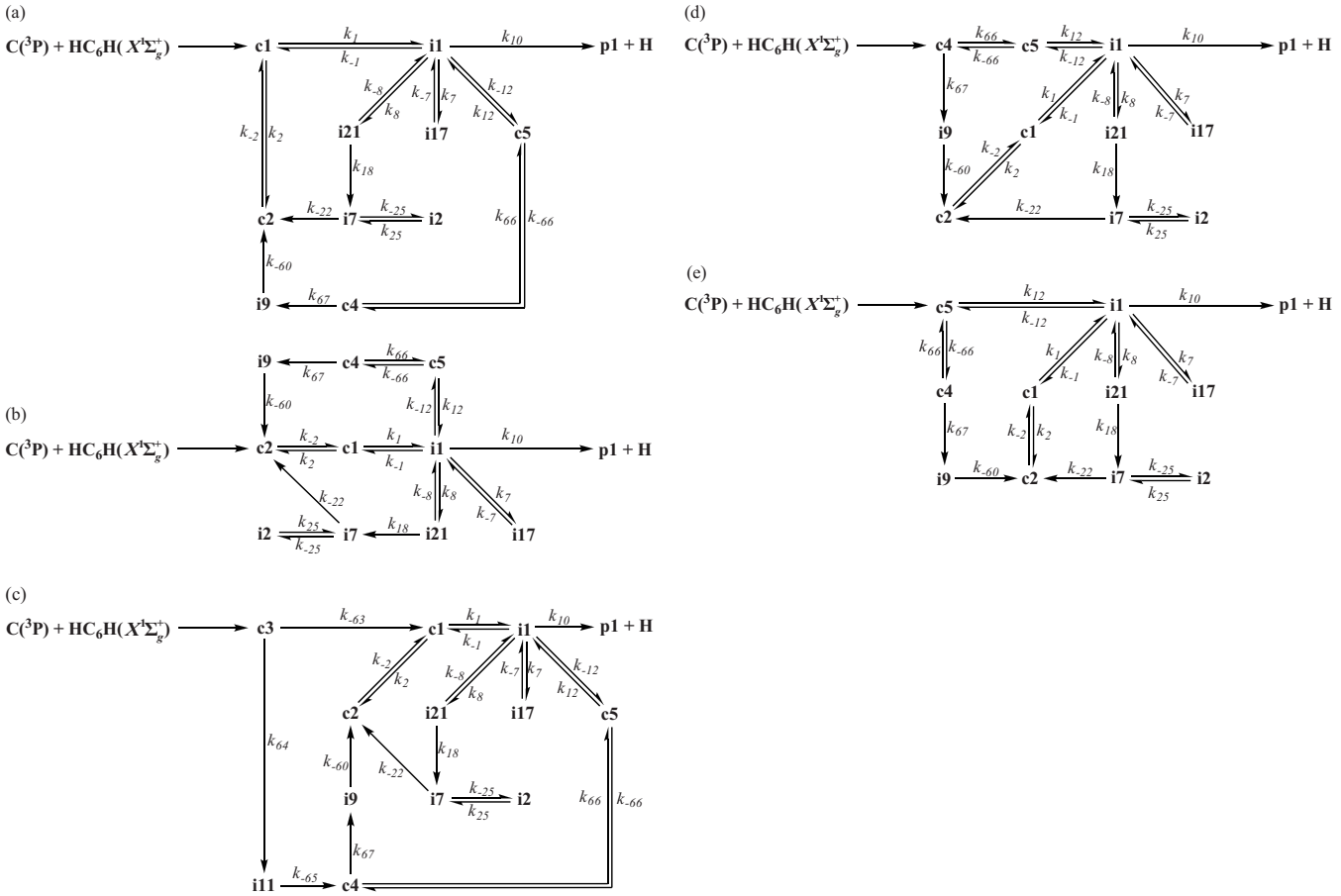

FIG. 8. The reaction mechanisms (a)–(e) derived from the most probable paths at 10 kcal/mol collision energy of collision complexes c1–c5, respectively, in which the k are the corresponding rate constants.

complexes, c2, c3, and c4 share the same fate of three-member ring closure, namely, the former two to c1 and the latest to c5, as already signified by negative energy barriers at CCSD(T)/cc-pVTZ level of calculations. Intriguingly, Fig. 7 clearly demonstrates that the reaction mechanism of c1 is a common theme for those of c2–c5, in which all collision complexes are inevitably trapped into the (c1, i1) loop before generating one single products: p1+H.

10 kcal/mol collision energy. The reaction mechanisms according to the most probable paths (Figs.[69] s8–s12) at collision energy of 10 kcal/mol are unveiled in Fig. 8. As the collision energy rises to 10 kcal/mol, k_{10} (i1→p1+H) advances significantly to edge k_9 (i1→i22) and k_{13} (i1→i36) out of the mechanism. Evidently, the route of c1 mechanism at 10 kcal/mol is persistently being the building block through out those of collision complexes c2–c5. With the exception of the c3 mechanism, in which i11 is also involved, the mechanisms of c1, c2, c4, and c5 even share the exact same course. Parallel to the counterparts at zero collision energy, i1 and p1 remain singularly important intermediate and product, respectively, in the mechanisms as the collision energy rises to 10 kcal/mol.

I. Evolution of concentrations with time

Zero collision energy. The rate equations for mechanisms of C+HC$_6$H reaction via collision complexes c1, c2, c3, c4, and c5 at zero collision energy as laid out in Figs. 10(a)–10(e) are solved numerically, in which the RRKM rate constants of Table I are adopted for these five sets of simultaneous differential equations in 9, 9, 11, 10, and 9 unknown concentrations, respectively. The evolution of concentrations with time thus obtained at zero collision energies for species in c1 reaction mechanism are shown in Fig. 9 and the ones for c2–c5 are in Fig. s13.[69]

Figure 9 demonstrates when the reaction of C+HC$_6$H proceeds via collision complex c1, in a fraction of a picosecond c1 simply dies down as its immediate isomers, c2 and i1 rise. c2 amounts to a healthy 0.155 of c1 initial concentration within a lifetime in subpicoseconds, i1 reaches peak concentration, 1.0, by 3.3 ps and stands firm well into submilliseconds. During this period, the decay of i1 to p1 is apparently slow enough that pre-equilibrium is established pairwisely between i1 and its immediate intermediates c5, i17, i21, i22, and i36, respectively, as evidenced by their peak concentrations duplicating fantastically the equilibrium values predicted by the corresponding ratios of forward and backward rate constants. Namely, with i1 concentration being 1, the equilibrium concentrations of c5, i17, i21, i22, and i36 are k_{-12}/k_{12}, k_7/k_{-7}, k_8/k_{-8}, k_9/k_{-9}, and k_{13}/k_{-13}, respectively, as inferred from Fig. 9, in which as listed in Table I, the rate constants responsible for returning to i1 are overwhelmingly large compared to the reversed and thus explain the dismal numbers for their peak concentrations. The lifetime of i1 nicely reflects the magnitude of its bottle-neck rate constant

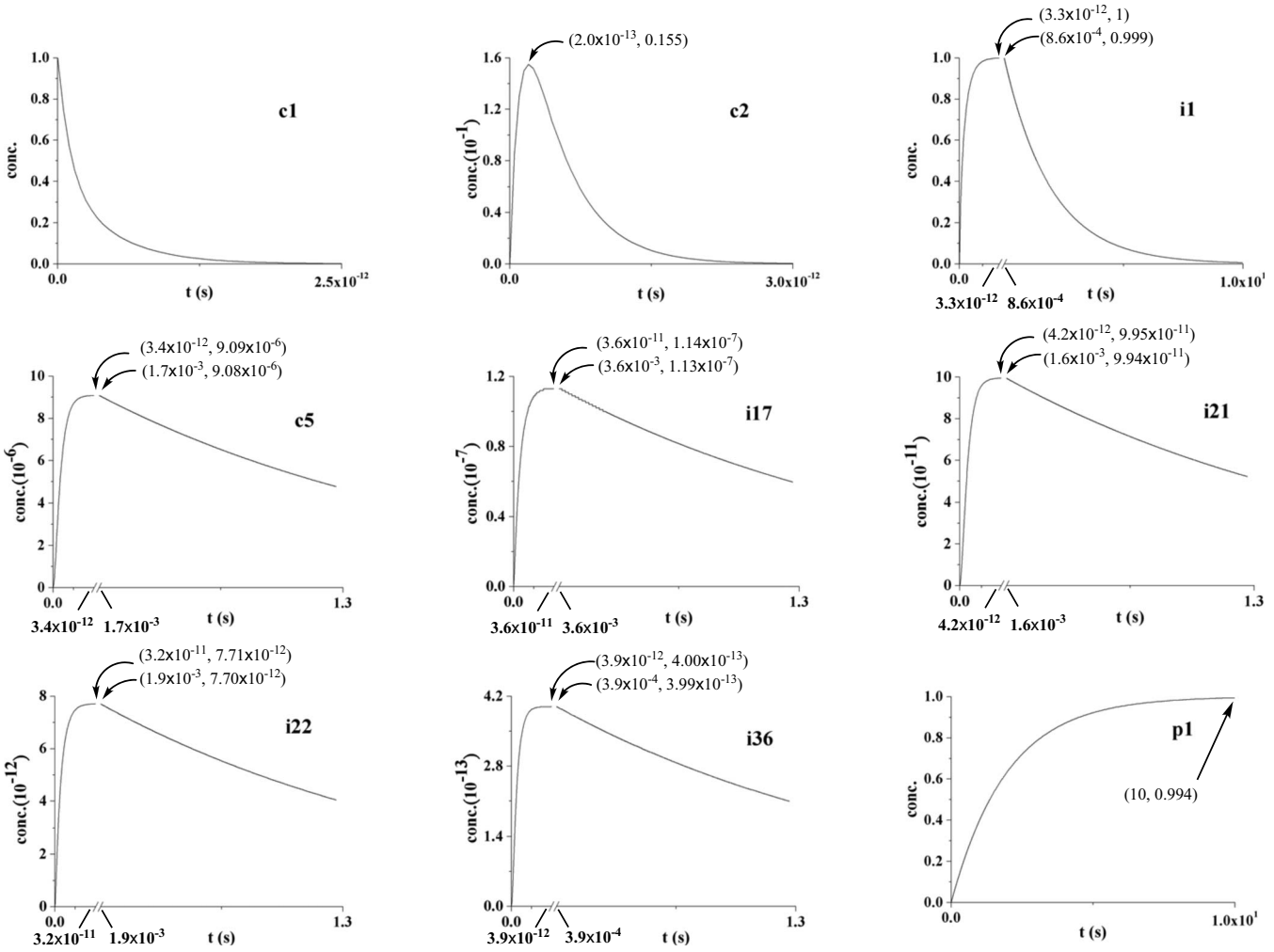

FIG. 9. The concentration evolution for each species in the c1 reaction mechanism at zero collision energy as in Fig. 7(a).

k_{10} of i1 → p1 + H. That is, i1 draining to the only products, p1 + H, or equivalently, the formation of p1, takes seconds to complete, which marks the end of the bimolecular reaction at a single-collision environment.

10 kcal/mol collision energy. Likewise, the rate equations for mechanisms of $C+HC_6H$ reaction via collision complexes c1, c2, c3, c4, and c5, respectively, at collision energy of 10 kcal/mol as laid out in Fig. 8(a)–8(e) are also solved, utilizing the RRKM rate constants at 10 kcal/mol in Table s2 for these five sets of simultaneous differential equations in 11, 11, 13, 11, and 11 unknown concentrations, respectively. The evolutions of concentrations with time are shown for the c1 mechanism Fig. 10, the rest are unveiled in Fig. s14.[69]

As illustrated in Fig. 10, for the $C+HC_6H$ proceeding through collision complex c1, the immediate intermediate c2 peaks to 0.176 rather early at subpicoseconds similar to the scenario for the zero collision energy; meanwhile c1 decays almost completely as i1 also reaches its maximum concentration, 1. The i1 retains its peak concentration until submicroseconds into the reaction when it starts to decay. During this period, the intermediates, c5, i17, i21, i7, i2, c4, and i9, also attain their respective peak concentrations that fascinatingly correlate precisely the predictions if the steady-state approximation were applied. For instance, according to the text book steady-state approximation, at steady state the concentration of c5 should follow that relation of $[c5]=(k_{66}[c4]+k_{-12}[i1])/(k_{-66}+k_{12})$ based on the mechanism in Fig. 8(a); knowing the peak concentrations of c4 and i1 being 4.75×10^{-6} and 1, respectively, the equation yields the c5 steady-state concentration, 2.07×10^{-5}, which reproduces exactly the c5 peak concentration indicated in Fig. 10. At the same time it explains clearly the fact that these seven intermediates never arise to detectable amounts. As simulated in Fig. 10 and anticipated from the magnitude of bottle-neck rate constant k_{10}, 1.01×10^{3} s^{-1}, the reaction would complete in a number of milliseconds when i1 dissociates to p1 + H entirely.

Implications for laboratory detection. The concentration revolutions at 0 and 10 kcal/mol imply that in subpicoseconds into the reaction, c1, c2, and i1 could be detected and within the typical detection time scale of microseconds for a crossed beam experiment, the observable species would be exclusively HC_7H (i1). As estimated from the k_{10} at 15 ~ 30 kcal/mol, C_7H (p1) could be detected comfortably when the collision energy is raised to at least 15 kcal/mol. It would be quite interesting to perform a crossed beam experiment at various collision energies to assess the validity of reaction mechanism we proposed.

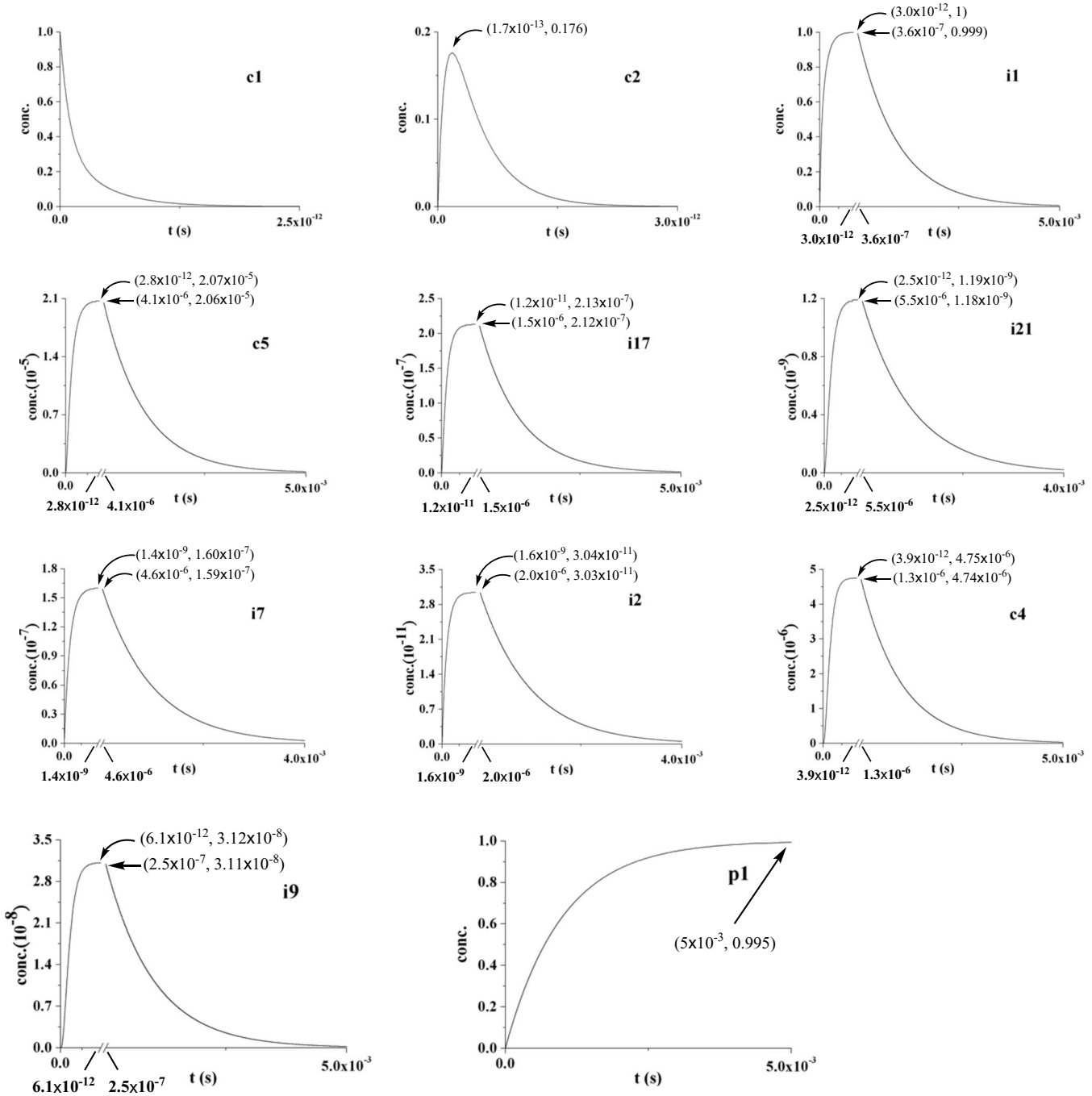

FIG. 10. The concentration evolution for each species in the c1 reaction mechanism at 10 kcal/mol collision energy as in Fig. 8(a).

J. Reaction cross sections

With the estimation of $\sigma_{c1}:\sigma_{c2}:\sigma_{c3}:\sigma_{c4}:\sigma_{c5}$ being 1.11: 1.24: 1.15: 1.13: 1, the statistic weight of 2 incorporated for c1–c4 due to symmetry yields 2.22: 2.48: 2.30: 2.26: 1. It implies that the overall reaction mechanism for $C(^3P)+HC_6H(X\ ^1\Sigma_g^+)$ is consisted of five mechanisms laid out in Figs. 7 and 8 with weights of (2.22, 2.48, 2.30, 2.26, 1).

K. Notes on C_7H_2 isomers

While it takes 38 C_5H_2 isomers in our study of $C+HC_4H$ reaction,[49] the number of relevant C_7H_2 isomers identified in this work escalates to 113, as paraded in Fig. 1 and s1,[69] the optimized structures for 5 collision complexes and 108 intermediates. Seven isomers have previously been predicted by theory: the singlet c1,[51,52,55] c5,[51,52,55] i1,[51,52] i7,[51,52] i64,[51,52] i65,[51,52,55,57] i98[51,52] and triplet c1,[52] c5,[52] i1,[28,51–56] i7,[52] i64,[52] i65,[52] and i98,[52] which leaves 106 newly found C_7H_2 isomers.

IV. CONCLUSION

Synthesis of interstellar radical C_7H via the reaction of ground state carbon atom, $C(^3P)$, and triacetylene, $HC_6H(X\ ^1\Sigma_g^+)$, has been investigated by combining *ab initio* electronic structure calculations for predicting reaction paths, subsequently RRKM theory to yield rate constant for each path, and a modified Langevin model for estimating captur-

TABLE I. Selected RRKM rate constants (s^{-1}) computed with B3LYP/6-311G(d,p) zero-point energy corrected CCSD(T)/cc-pVTZ energies, and B3LYP/6-311G(d,p) harmonic frequencies at collision energies of 0.0, 0.03, 0.15, 2.0, 5.0, and 10.0 kcal/mol.

	0.0	0.03	0.15	2.0	5.0	10.0
k_7 (i1→i17)	1.99×10^{4}	2.00×10^{4}	2.05×10^{4}	2.93×10^{4}	5.02×10^{4}	1.12×10^{5}
k_{-7} (i17→i1)	1.75×10^{11}	1.76×10^{11}	1.78×10^{11}	2.24×10^{11}	3.17×10^{11}	5.26×10^{11}
k_8 (i1→i21)	2.16×10^{2}	2.18×10^{2}	2.27×10^{2}	4.20×10^{2}	1.04×10^{3}	3.84×10^{3}
k_{-8} (i21→i1)	2.17×10^{12}	2.17×10^{12}	2.18×10^{12}	2.29×10^{12}	2.46×10^{12}	2.71×10^{12}
k_9 (i1→i22)	1.72	1.74	1.85	4.29	1.45×10^{1}	7.93×10^{1}
k_{-9} (i22→i1)	2.23×10^{11}	2.24×10^{11}	2.30×10^{11}	3.24×10^{11}	5.17×10^{11}	9.51×10^{11}
k_{10} (i1→p1+H)	5.11×10^{-1}	5.30×10^{-1}	6.08×10^{-1}	4.09	4.74×10^{1}	1.01×10^{3}
k_{12} (c5→i1)	3.53×10^{12}	3.53×10^{12}	3.54×10^{12}	3.71×10^{12}	3.97×10^{12}	4.39×10^{12}
k_{-12} (i1→c5)	3.21×10^{7}	3.22×10^{7}	3.27×10^{7}	4.05×10^{7}	5.61×10^{7}	9.20×10^{7}
k_{13} (i1→i36)	2.03	2.06	2.18	5.27	1.87×10^{1}	1.09×10^{2}
k_{-13} (i36→i1)	5.08×10^{12}	5.09×10^{12}	5.12×10^{12}	5.53×10^{12}	6.14×10^{12}	6.98×10^{12}
k_{66} (c4→c5)	2.45×10^{12}	2.45×10^{12}	2.45×10^{12}	2.44×10^{12}	2.44×10^{12}	2.44×10^{12}
k_{-66} (c5→c4)	2.71×10^{11}	2.72×10^{11}	2.75×10^{11}	3.26×10^{11}	4.18×10^{11}	6.04×10^{11}

ing cross sections. Navigating with the guide of RRKM rate constants through the intricate web of *ab initio* reactions paths, which are composed of 5 collision complexes, 108 intermediates, 20 H-dissociated products, and the corresponding transition states, the most probable paths drastically distilled to around ten species at collision energies of 0 and 10 kcal/mol, respectively, are identified and adopted as the reaction mechanisms. The rate equations for the reaction mechanisms are solved numerically such that the evolutions of concentrations with time are obtained. It is fascinating to find that the phenomena of pre-equilibrium and steady-state occur at 0 and 10 kcal/mol, respectively, and their periods are timed exactly in our calculations. Overall, 106 C_7H_2 and 16 C_7H isomers are newly found in this work.

This study predicts that five collision complexes, c1, c2, c3, c4, and c5, would end up at one single final products, linear C_7H (p1)+H, via the most stable intermediate, linear HC_7H (i1). The concentration evolutions predict that for a crossed beam experiment performed at collision energy of 0–10 kcal/mol, HC_7H (i1) could be captured, and C_7H (p1) would be detectable when the collision energy is elevated to 15 kcal/mol and higher. The first member of interstellar reaction class, $C(^3P)+C_2H_2\rightarrow C_3H+H$, is famously known to form both linear and cyclic C_3H isomers with the latter being lower in energy, as the second member, reaction of carbon atom with the first polyyne, diacetylene, $C(^3P)+HC_4H\rightarrow C_5H+H$ is found to produce only the carbon chain C_5H, the most stable isomer. The present work confirms that for the third member, the mechanism, $C(^3P)+HC_6H\rightarrow HC_7H\rightarrow C_7H+H$, holds, which substantiates effectively that the reaction of a carbon atom with polyyne $HC_{2n}H$ would yield a carbon chain $C_{2n+1}H$ through a linear $HC_{2n+1}H$ intermediate, $C(^3P)+HC_{2n}H\rightarrow HC_{2n+1}H\rightarrow C_{2n+1}H+H$. Our investigation indicates that the $C(^3P)+HC_6H(X\ ^1\Sigma_g^+)$ reaction would be an efficient route for triacetylene depletion and C_7H ($X\ ^2\Pi$) formation in interstellar medium. Therefore, the barrierless and exoergic reaction of ground state carbon atoms with triacetylene presents a compelling route to synthesize C_7H ($X\ ^2\Pi$) in cold molecular clouds.

ACKNOWLEDGMENTS

Computer resources at the National Center for High-performance Computer of Taiwan were utilized in the calculations. R.I.K. thanks the U.S. National Science Foundation via the *Collaborative Research in Chemistry* Program No. NSF-CRC CHE-0627854.

[1] H. S. P. Muller, S. Thorwirth, D. A. Roth, and G. Winnerwisser, Astron. Astrophys. **370**, L49 (2001) http://www.cdms.de.
[2] M. B. Bell, P. A. Feldman, M. J. Travers, M. C. McCarthy, C. A. Gottlieb, and P. Thaddeus, Astrophys. J. **483**, L61 (1997).
[3] B. E. Turner, Astrophys. J. **163**, L35 (1971).
[4] M. Morris, W. Gilmore, P. Palmer, B. E. Turner, and B. Zuckerman, Astrophys. J. **199**, L47 (1975).
[5] N. W. Broten, T. Oka, L. W. Avery, J. M. MacLeod, and H. W. Kroto, Astrophys. J. **223**, L105 (1978).
[6] H. W. Kroto, C. Kirby, D. R. M. Walton, L. W. Broten, J. M. MacLead, and T. Oka, Astrophys. J. **219**, L133 (1978).
[7] O. E. H. Rydbeck, J. Ellder, and W. M. Irvine, Nature (London) **246**, 466 (1973).
[8] K. D. Tucker, M. L. Kutner, and P. Thaddeus, Astrophys. J. **193**, L115 (1974).
[9] P. Thaddeus, C. A. Gottlieb, A. Hjalmarson, L. E. B. Johannson, W. M. Irvine, P. Friberg, and R. A. Linke, Astrophys. J. **294**, L49 (1985).
[10] M. Guelin, S. Green, and P. Thaddeus, Astrophys. J. **224**, L27 (1978).
[11] J. Cernicharo, C. Kahane, J. Gomez-Gonzalez, and M. Guelin, Astron. Astrophys. **164**, L1 (1986).
[12] H. Suzuki, M. Ohishi, N. Kaifu, S. I. Ishikawa, and T. Kasuga, Publ. Astron. Soc. Jpn. **38**, 911 (1986).
[13] M. Guelin, J. Cernicharo, M. J. Travers, M. C. McCarthy, C. A. Gottlieb, P. Thaddeus, M. Ohishi, S. Saito, and S. Yamamoto, Astron. Astrophys. **317**, L1 (1997).
[14] J. Cernicharo and M. Guelin, Astron. Astrophys. **309**, L27 (1996).
[15] J. Cernicharo, A. M. Heras, A. G. G. M. Tielens, J. R. Pardo, F. Herpin, M. Guelin, and L. B. F. M. Waters, Astrophys. J. **546**, L123 (2001).
[16] J. Cernicharo, C. A. Gottlieb, M. Guelin, T. C. Killian, G. Paubert, P. Thaddeus, and J. M. Vrtilek, Astrophys. J. **368**, L39 (1991).
[17] J. Cernicharo, C. A. Gottlieb, M. Guelin, T. C. Killian, P. Thaddeus, and J. M. Vrtilek, Astrophys. J. **368**, L43 (1991).
[18] W. D. Langer, T. Velusamy, T. B. H. Kuiper, R. Peng, M. C. McCarthy, M. J. Travers, A. Kovacs, C. A. Gottlieb, and P. Thaddeus, Astrophys. J. **480**, L63 (1997).
[19] M. C. McCarthy, M. J. Travers, A. Kovacs, W. Chen, S. E. Novick, C. A. Gottlieb, and P. Thaddeus, Science **275**, 518 (1997).
[20] M. C. McCarthy, M. J. Travers, A. Kovacs, C. A. Gottlieb, and P. Thaddeus, Astrophys. J., Suppl. Ser. **113**, 105 (1997).
[21] A. J. Apponi, M. C. McCarthy, C. A. Gottlieb, and P. Thaddeus, Astrophys. J. **530**, 357 (2000).

[22] A. E. Douglas, Nature (London) **269**, 130 (1977).
[23] J. Fulara, D. Lessen, P. Frelvogel, and J. P. Maier, Nature (London) **366**, 439 (1993).
[24] G. H. Herbig, Annu. Rev. Astron. Astrophys. **33**, 19 (1995).
[25] T. Pinto, H. Ding, F. Guthe, and J. P. Maier, J. Chem. Phys. **114**, 2208 (2001).
[26] C. D. Ball, M. C. McCarthy, and P. Thaddeus, Astrophys. J. **523**, L89 (1999).
[27] C. D. Ball, M. C. McCarthy, and P. Thaddeus, J. Chem. Phys. **112**, 10149 (2000).
[28] H. Ding, T. W. Schmidt, T. Pinto, A. E. Boguslavskiy, F. Guthe, and J. P. Maier, J. Chem. Phys. **119**, 814 (2003).
[29] M. Kotterer and J. P. Maier, Chem. Phys. Lett. **266**, 342 (1997).
[30] H. Linnartz, T. Motylewski, O. Vaizert, J. P. Maier, A. J. Apponi, M. C. McCarthy, C. A. Gottlieb, and P. Thaddeus, J. Mol. Spectrosc. **197**, 1 (1999).
[31] H. Linnartz, T. Motylewski, and J. P. Maier, J. Chem. Phys. **109**, 3819 (1998).
[32] H. Ding, T. Pino, F. Guthe, and J. P. Maier, J. Chem. Phys. **117**, 8362 (2002).
[33] A. Dzhonson, E. B. Jochnowitz, E. Kim, and J. P. Maier, J. Chem. Phys. **126**, 044301 (2007).
[34] K. Hoshina, H. Kohguchi, Y. Ohshima, and Y. Endo, J. Chem. Phys. **108**, 3465 (1998).
[35] M. L. Heger, Lick Obs. Bull. **10**, 146 (1922).
[36] T. Allain, S. Leach, and E. Sedlmayr, Astron. Astrophys. **305**, 602 (1995).
[37] J. P. Maier, J. Phys. Chem. A **102**, 3462 (1998).
[38] M. Tulej, D. A. Kirkwood, M. Pachkov, and J. P. Maier, Astrophys. J. **506**, L69 (1998).
[39] B. J. McCall, J. Thorburn, L. M. Hobbs, T. Oka, and D. G. York, Astrophys. J. **559**, L49 (2001).
[40] G. Galazutdinov, F. Musaev, J. Nirski, and J. Krelowski, Astron. Astrophys. **377**, 1063 (2001).
[41] E. Herbst, H. H. Lee, D. A. Howe, and T. J. Millar, Mon. Not. R. Astron. Soc. **268**, 335 (1994).
[42] R. P. Bettens, H. H. Lee, and E. Herbst, Astrophys. J. **443**, 664 (1995).
[43] R. P. Bettens and E. Herbst, Astrophys. J. **468**, 686 (1996).
[44] T. J. Millar, P. R. A. Farquhar, and K. Willacy, Astron. Astrophys. **121**, 139 (1997).
[45] R. I. Kaiser, C. Ochsenfeld, M. Head-Gordon, and Y. T. Lee, Science **274**, 1508 (1996).
[46] D. C. Clary, E. Buonomo, I. R. Sims, I. W. M. Smith, W. D. Geppert, C. Naulin, M. Costes, L. Cartechini, and P. Casavecchia, J. Phys. Chem. A **106**, 5541 (2002) (and the references therein.).
[47] E. Herbst, Chem. Soc. Rev. **30**, 168 (2001).
[48] R. I. Kaiser, Chem. Rev. (Washington, D.C.) **102**, 1309 (2002).
[49] B. J. Sun, C. Y. Huang, H. H. Kuo, K. T. Chen, H. L. Sun, C. H. Huang, M. F. Tsai, C. H. Kao, Y. S. Wang, L. G. Gao, R. I. Kaiser, and A. H. H. Chang, J. Chem. Phys. **128**, 244303 (2008).
[50] F. T. Zhang, Y. S. Kim, L. Zhou, R. I. Kaiser, and A. H. H. Chang, J. Chem. Phys. **129**, 134313 (2008).
[51] D. L. Cooper and S. C. Murphy, Astrophys. J. **333**, 482 (1988).
[52] S. Dua, S. J. Blanksby, and J. H. Bowie, J. Phys. Chem. A **104**, 77 (2000).
[53] Q. Fan and G. V. Pfeiffer, Chem. Phys. Lett. **162**, 472 (1989).
[54] C. Zhang, Z. Cao, H. Wu, and Q. Zhang, Int. J. Quantum Chem. **98**, 299 (2004).
[55] K. Aoki and S. Ikuta, J. Mol. Struct.: THEOCHEM **310**, 229 (1994).
[56] G. Mpourmpakis, M. Muhlhauser, G. E. Froudakis, and S. D. Peyerimhoff, Chem. Phys. Lett. **356**, 398 (2002).
[57] S. A. Maluendes and A. D. McLean, Chem. Phys. Lett. **200**, 511 (1992).
[58] J. Takahashi, Publ. Astron. Soc. Jpn. **52**, 401 (2000).
[59] D. E. Woon, Chem. Phys. Lett. **244**, 45 (1995).
[60] A. D. Becke, J. Chem. Phys. **98**, 5648 (1993); **96**, 2155 (1992); **97**, 9173 (1992); C. Lee, W. Yang, and R. G. Parr, Phys. Rev. B **37**, 785 (1988).
[61] G. D. Purvis and R. J. Bartlett, J. Chem. Phys. **76**, 1910 (1982); C. Hampel, K. A. Peterson, and H.-J. Werner, Chem. Phys. Lett. **190**, 1 (1992); P. J. Knowles, C. Hampel, and H.-J. Werner, J. Chem. Phys. **99**, 5219 (1993); M. J. O. Deegan and P. J. Knowles, Chem. Phys. Lett. **227**, 321 (1994).
[62] M. J. Frisch, G. W. Trucks, H. B. Schlegel, *et al.*, GAUSSIAN 98, Revision A.5, Gaussian, Inc., Pittsburgh, PA, 1998; GAUSSIAN 03, Revision C.02, Gaussian, Inc., Wallingford CT, 2004.
[63] H. Eyring, S. H. Lin, and S. M. Lin, *Basic Chemical Kinetics* (Wiley, New York, 1980).
[64] A. H. H. Chang, A. M. Mebel, X.-M. Yang, S. H. Lin, and Y. T. Lee, J. Chem. Phys. **109**, 2748 (1998).
[65] W. L. Hase, Acc. Chem. Res. **16**, 258 (1983).
[66] R. A. Marcus, Chem. Phys. Lett. **144**, 208 (1988).
[67] A. H. H. Chang, D. W. Hwang, X. M. Yang, A. M. Mebel, S. H. Lin, and Y. T. Lee, J. Chem. Phys. **110**, 10810 (1999).
[68] R. D. Levine and R. B. Bernstein, *Molecular Reaction Dynamics and Chemical Reactivity* (Oxford University Press, New York, 1987).
[69] See EPAPS supplementary material at http://dx.doi.org/10.1063/1.3212625 for Tables s1, s2, and Figures s1–s14.